# Electronic Supplementary Information (ESI)

## Validation of potential function

In order to identify the validity of this simulated study, it is need to validate the used potential functions. Here, the indentation hardness (H) of monocrystalline Cu is calculated using equation (1, 2) and compared with other research in Table 2. In the equations, $P_{max}$ is the peak load, $A_c$ is the projected contact area, and $d$ is the diameter of spherical indenter under the peak indentation depth.

$$H = \frac{P_{\max}}{A_c} \tag{1}$$

$$A_c = \frac{\pi d^2}{4} \tag{2}$$

**Table S1.** Comparison of hardness values for nanoindentation without water film.

| Hardness/GPa | | Conditions | |
|---|---|---|---|
| This work | 12.67 | Cu (001), indentation hardness | |
| simulation | 12.0 | Cu (100), indentation hardness | [1] |
| | 18.031 | Cu (010) after indentation | [2] |
| | 12.3 | Cu (111), indentation hardness | [3] |
| experiment | 6.0 | Cu | [4] |
| | 2.7~8.0 | Cu film with 400nm, with increasing indentation depth | [5] |
| | 2.27~3.35 | Cu thin film thickness 500~100nm | [6] |

From this table, we can find that the value of hardness from simulated research is much larger than that from experimental research, which maybe is attributed to the anisotropy of copper substrate. However, the hardness in our study is similar to other simulated results. Thus, we consider that the EAM potential and Morse potential used in our work are accurate to investigate the nanoindentation behavior of monocrystalline Cu.

The rigid TIP4P model comprised of three fixed point charges and one Lennard-Jones center is applied to simulate the condensed phase of water film, which has been

validated by a lot of research. [7, 8] The Cu-O and C-O interactions are described by Lennard-Jones (12-6) potential, and Lorentz-Berthelot mixing rules are employed to obtain the relevant parameters. [7, 9-11] Therefore, we think our simulated work is accurate enough to elucidate the nanoindentation property.

**Load-depth curves and dislocation evolution processes**

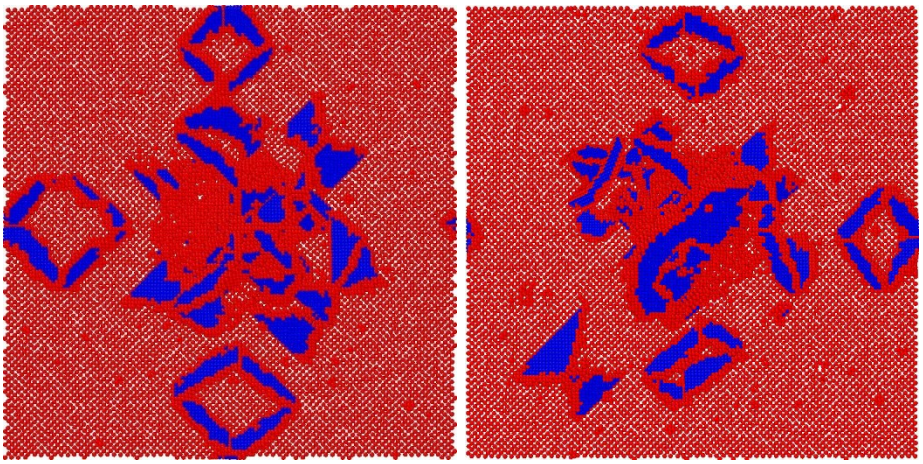

(a) H=3 nm (b) H=4 nm

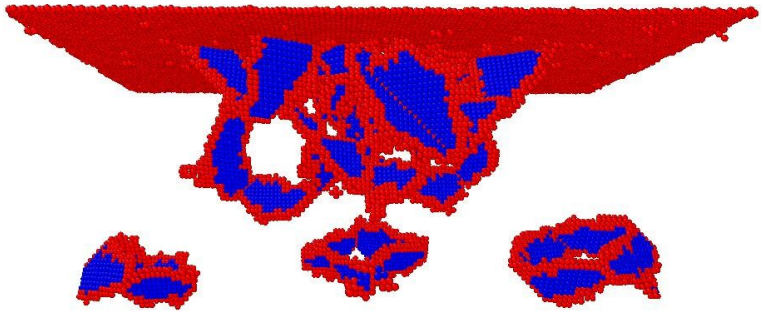

(c) H=3 nm

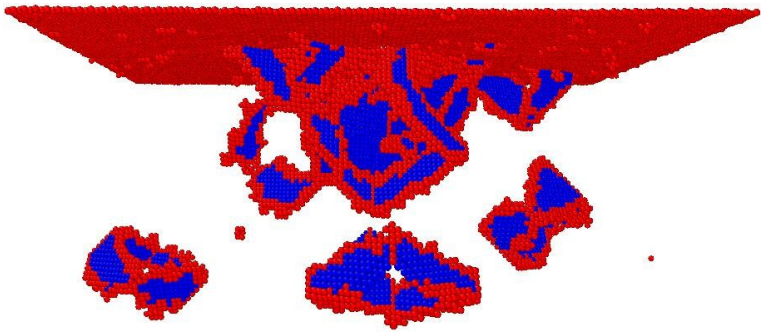

(d) H=4 nm

**Fig. S1.** Dislocation structure at end of loading for water film thickness of 3 nm and 4 nm, (a) and (b) view from bottom, (c) and (d) view from front of Cu substrate. Red represents the surface and dislocation atoms and blue represents stacking fault.

**Discussion on the plastic deformation mechanism**

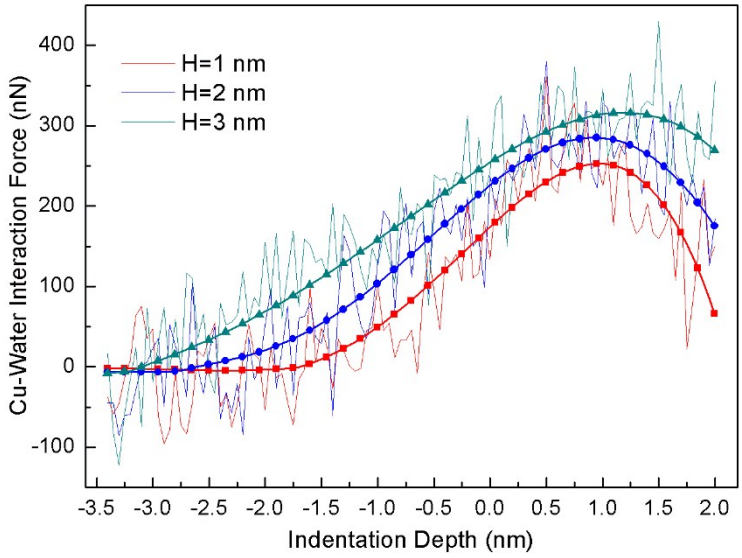


**Fig. S2.** The interaction force between water film and monocrystal Cu with different water film thickness (H). The line-symbol curves is the fitted curves corresponding to the same color straight-line curves.

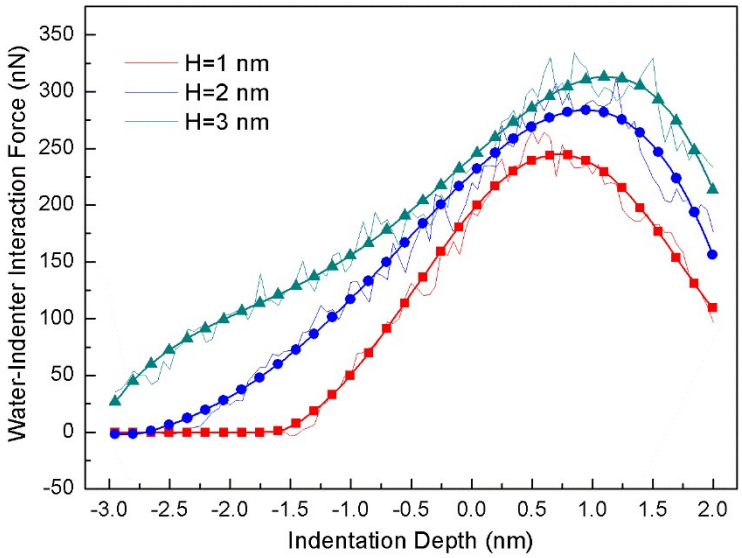


**Fig. S3.** The interaction force between water film and indenter with different water film thickness (H). The line-symbol curves is the fitted curves corresponding to the same color straight-line curves.

The relative error (*Er*) between the interaction force of indenter-water film and that of Cu workpiece-water film with different water film thickness is calculated using the following equation, shown in Table S1 and Fig. S1.

$$Er = \left| \frac{Interaction_{Cu-H_2O} - Interaction_{C-H_2O}}{Interaction_{C-H_2O}} \right| \times 100\%$$

**Table S2.** The relative error (*Er*) between the interaction force of indenter-water film and that of Cu workpiece-water film with different water film thickness.

| Depth /nm | -1.0 | -0.5 | 0 | 0.5 | 1.0 | 1.5 | 2.0 |
|---|---|---|---|---|---|---|---|
| H=1 nm | 0.78% | 11.27% | 9.44% | 3.86% | 7.26% | 12.89% | 30.48% |
| H=2 nm | 11.4% | 4.31% | 8.17% | 0.78% | 0.50% | 0.89% | 0.92% |
| H=3 nm | 1.41% | 6.00% | 9.77% | 2.44% | 0.85% | 4.14% | 14.70% |

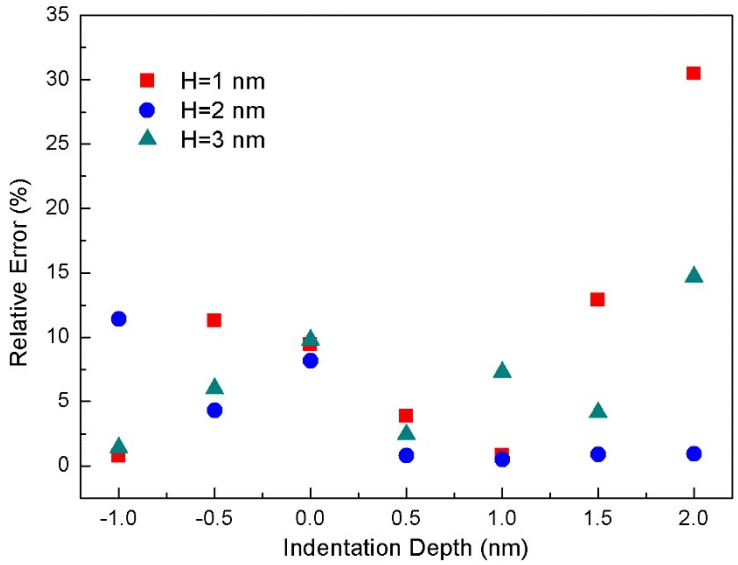


**Fig. S4.** The relative error between the interaction force of indenter-water film and that of Cu workpiece-water film with different water film thickness.

**Reference:**


[1] G. Ziegenhain, H. M. Urbassek, A. Hartmaier. *J. Appl. Phys.* 107 (2010) 061807.

[2] L. Q. Li, W. P. Song, M. Wu, A. Ovcharenko, G. Y. Zhang. *Comp. Mater. Sci*. 98 (2015) 105–111.

[3] K. Sun, W. T. Shen, L. F. Ma. *Comp. Mater. Sci*. 81 (2014) 226–232.

[4] M. Göken, M. Kempf. *Z. Metallkd*. 92 (2001) 1061.

[5] D. Beegan, S. Chowdhury, M. T. Laugier. *Surf. Coat. Tech*. 192 (2005) 57–63.

[6] D. Beegan, S. Chowdhury, M. T. Laugier. *Surf. Coat. Tech.*, 201 (2007) 5804–5808.

[7] J. Ren, J. Zhao, Z. Dong, P. Liu. *App. Surf. Sci.* 346 (2015) 84–98.

[8] J.L.F. Abascal, C. Vega. *J. Chem. Phys*. 123 (2005) 234505.

[9] D. Boda, D. Henderson. *Mol. Phys.* 106 (2008) 2367–2370.

[10] A.K. Al-Matar, D.A. Rockstraw. *J. Comput. Chem*. 25 (2003) 660–668.

[11] T. Werder, J.H. Walther, R.L. Jaffe, T. Halicioglu, P. Koumoutsakos. *J. Phys. Chem. B* 107 (2003) 1345–1352.